

AD_____

Award Number: DAMD17-99-1-9493

TITLE: Pro-Apoptotic Changes in Brain Mitochondria After Toxic Exposure

PRINCIPAL INVESTIGATOR: Thomas J. Sick, Ph.D.

CONTRACTING ORGANIZATION: University of Miami
Miami, Florida 33136

REPORT DATE: July 2001

TYPE OF REPORT: Annual

PREPARED FOR: U.S. Army Medical Research and Materiel Command
Fort Detrick, Maryland 21702-5012

DISTRIBUTION STATEMENT: Approved for Public Release;
Distribution Unlimited

The views, opinions and/or findings contained in this report are those of the author(s) and should not be construed as an official Department of the Army position, policy or decision unless so designated by other documentation.

20020107 049

REPORT DOCUMENTATION PAGE			Form Approved OMB No. 074-0188	
Public reporting burden for this collection of information is estimated to average 1 hour per response, including the time for reviewing instructions, searching existing data sources, gathering and maintaining the data needed, and completing and reviewing this collection of information. Send comments regarding this burden estimate or any other aspect of this collection of information, including suggestions for reducing this burden to Washington Headquarters Services, Directorate for Information Operations and Reports, 1215 Jefferson Davis Highway, Suite 1204, Arlington, VA 22202-4302, and to the Office of Management and Budget, Paperwork Reduction Project (0704-0188), Washington, DC 20503				
1. AGENCY USE ONLY (Leave blank)	2. REPORT DATE July 2001	3. REPORT TYPE AND DATES COVERED Annual (1 Jul 00 - 30 Jun 01)		
4. Pro-Apoptotic Changes in Brain Mitochondria After Toxic Exposure		5. FUNDING NUMBERS DAMD17-99-1-9493		
6. AUTHOR(S) Thomas J. Sick, Ph.D.				
7. PERFORMING ORGANIZATION NAME(S) AND ADDRESS(ES) University of Miami Miami, Florida 33136 E-Mail: tsick@miami.edu		8. PERFORMING ORGANIZATION REPORT NUMBER		
9. SPONSORING / MONITORING AGENCY NAME(S) AND ADDRESS(ES) U.S. Army Medical Research and Materiel Command Fort Detrick, Maryland 21702-5012		10. SPONSORING / MONITORING AGENCY REPORT NUMBER		
11. SUPPLEMENTARY NOTES Report contains color				
12a. DISTRIBUTION / AVAILABILITY STATEMENT Approved for Public Release; Distribution Unlimited			12b. DISTRIBUTION CODE	
13. ABSTRACT (Maximum 200 Words) Mitochondria normally function to provide sources of energy for vital cellular functions. However, under stressful conditions these organelles may trigger events that lead eventually to cell death. Thus, mitochondria have been implicated as major contributors to neuronal death in a variety of neurodegenerative disorders. In this report we provide evidence that certain mitochondrial toxins cause selective cell death in hippocampal subfield CA1 that has previously been shown to be selectively vulnerable to hypoxia/ischemia. We have also measured changes in mitochondrial membrane potential following toxin exposure. Little mitochondrial depolarization was observed at times when electrophysiology was compromised. Finally, we provide preliminary evidence of redistribution of cytochrome c following toxin exposure. This redistribution was seen primarily in hippocampal subfield CA1 and in the dentate gyrus. Activation of Caspase-3 was only observed in the dentate gyrus, suggesting that activation of this pro-apoptotic factor may not be responsible for cell death in the CA1 subfield.				
14. SUBJECT TERMS Neurotoxin			15. NUMBER OF PAGES 22	
			16. PRICE CODE	
17. SECURITY CLASSIFICATION OF REPORT Unclassified	18. SECURITY CLASSIFICATION OF THIS PAGE Unclassified	19. SECURITY CLASSIFICATION OF ABSTRACT Unclassified	20. LIMITATION OF ABSTRACT Unlimited	

FOREWORD

Opinions, interpretations, conclusions and recommendations are those of the author and are not necessarily endorsed by the U.S. Army.

N/A Where copyrighted material is quoted, permission has been obtained to use such material.

N/A Where material from documents designated for limited distribution is quoted, permission has been obtained to use the material.

N/A Citations of commercial organizations and trade names in this report do not constitute an official Department of Army endorsement or approval of the products or services of these organizations.

X^{TS} In conducting research using animals, the investigator(s) adhered to the "Guide for the Care and Use of Laboratory Animals," prepared by the Committee on Care and use of Laboratory Animals of the Institute of Laboratory Resources, national Research Council (NIH Publication No. 86-23, Revised 1985).

N/A For the protection of human subjects, the investigator(s) adhered to policies of applicable Federal Law 45 CFR 46.

N/A In conducting research utilizing recombinant DNA technology, the investigator(s) adhered to current guidelines promulgated by the National Institutes of Health.

N/A In the conduct of research utilizing recombinant DNA, the investigator(s) adhered to the NIH Guidelines for Research Involving Recombinant DNA Molecules.

N/A In the conduct of research involving hazardous organisms, the investigator(s) adhered to the CDC-NIH Guide for Biosafety in Microbiological and Biomedical Laboratories.

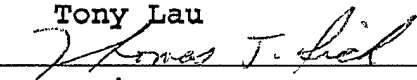
Tony Lau

PI - Signature 7/30/01
Date

Table of Contents

Front cover	1
Report Documentation Page	2
Foreward	3
Table of Contents	4
Introduction	5
Body	5
Key Research Accomplishments	9
Reportable Outcomes	9
Conclusions	9
Appendices	10

Introduction

The work funded by this contract continues to examine the functional changes in brain mitochondria associated with exposure to mitochondrial toxins, and to determine whether these changes are compatible with neuronal survival, acute neuronal dysfunction or known signals of delayed or apoptotic cell death. The goals are: 1) to first characterize toxin-induced alterations of respiratory chain redox status and mitochondrial membrane potential in intact functioning neuronal populations, and to assess the reversibility of acute toxin exposure in terms of mitochondrial and neuronal function; 2) to examine the role of specific intracellular mediators of mitochondrial and neuronal dysfunction including release of mitochondrial cytochrome *c*, calcium overload, reactive oxygen species (ROS), and mitochondrial permeability transition. Experiments conducted to date utilized brain slice preparations for monitoring mitochondrial redox activities, mitochondrial membrane potential ($\Delta\psi_m$) and electrical function. Rapid scanning spectrophotometry and spectrofluorometry was used to assess mitochondrial function, while microelectrode electrophysiology was used to evaluate neuronal function.

Body

In the first year of this contract, we began analysis of the electrophysiological and mitochondrial functional changes associated with exposure of hippocampal slices to a variety of neurotoxins including the 1-methyl-4-phenylpyridium (MPP⁺) and 3-nitropropionic acid (3-NP). We also described the development of a new organotypic hippocampal slice culture model which would be employed to study long-term effects of toxin exposure including markers of cell death. In this report, we present data completing the initial analysis of the effects of toxins on mitochondrial NADH and electrophysiology including the effects of the excitotoxin N-methyl-D-aspartate (NMDA) and the pesticide rotenone. Although rotenone was not initially included for analysis as part of this contract, we have included this agent because this mitochondrial Complex I inhibitor has recently been shown to cause selective nigral-striatal damage following systemic administration in rodents. In this report, we also present data showing the effects of toxin exposure on neuronal viability in our organotypic slice culture model. In year 2, we have also begun analysis of toxin exposure on pro-apoptotic changes in brain mitochondria including changes in mitochondrial membrane potential and cytochrome *c*. These studies are describe in detail below.

1) Effects of NMDA on mitochondrial NADH and synaptic transmission in hippocampal slices.

In these experiments, hippocampal slices were exposed for 60 min to either artificial cerebrospinal fluid (ACSF), 10 μ M NMDA, 50 μ M NMDA, or 100 μ M NMDA. Evoked post-synaptic potentials were recorded in subfield CA1 following electrical stimulation of the Schafer collaterals. Mitochondrial NADH redox activity was also measured in CA1 using laser excitation (337 nm) and fiberoptic measurement of emitted NADH fluorescence.

The data are summarized in Figures 1 and 2, which respectively show the effects of NMDA exposure on evoked potentials and mitochondrial NADH fluorescence in hippocampal subfield CA1. Exposure of hippocampal slices to 10 μ M NMDA had little effect on either evoked electrical activity or NADH fluorescence in hippocampal slices. Exposure to 50 μ M or 100 μ M NMDA resulted in a decrease in mitochondrial NADH fluorescence and inhibition of evoked electrical activity. The decrease in NADH fluorescence indicates oxidation of this respiratory chain electron donor.

It is not clear at present whether NMDA-induced oxidation of NADH represents primary mitochondrial toxicity or a secondary mitochondrial response to NMDA receptor activation. For example, NMDA-induced elevation of intracellular calcium ion levels would be expected to stimulate respiration and decrease the NADH/NAD⁺ ratio. Likewise, inhibition of key citric acid cycle enzymes by elevation of intracellular calcium ion might also inhibit mitochondrial production of NADH. Future studies will be required to sort out these possibilities.

2) Effects of rotenone on mitochondrial NADH and synaptic transmission in hippocampal slices

Rotenone is a pesticide that inhibits Complex I of the mitochondrial respiratory chain and causes degeneration of nigral-striatal neurons in rodents. We tested the effect of rotenone on mitochondrial NADH and electrophysiology in hippocampal slices. The data are shown in Figures 3 and 4. Rotenone treatment resulted in a dose-dependent decline in evoked potential amplitude in hippocampal subfield CA1. This change in hippocampal electrophysiology was similar to that observed for MPP⁺ and other toxins tested. However, there appeared to be a significant difference in the response of mitochondrial NADH to rotenone and MPP⁺, although both inhibit Complex I activity. Rotenone had little effect on steady state levels of NADH, yet completely inhibited further reduction of NADH upon removal of oxygen (Figure 4). As reported in our previous report, MPP⁺ treatment resulted in increased reduced/oxidized NADH but did not inhibit further reduction upon removal of oxygen (Figure 5). Thus, although both toxins inhibit Complex I of the respiratory chain, the mechanism of inhibition appears to be different.

3) Cell viability of organotypic hippocampal slice cultures after toxin exposure.

Organotypic hippocampal slice cultures were exposed for 1 hr to MPP⁺, rotenone, 3-NP, or NMDA. Cell death was estimated by fluorescence imaging after propidium iodide 1 day, 2 days, or 3 days after toxin treatment. Propidium iodide fluoresces upon reaction with nucleic acids. This reaction occurs in cells lacking both plasma membrane and nuclear membrane integrity and thus signals cell death. In these experiments, we compared toxicity in hippocampal subfields CA1 and CA3 since these regions have been previously shown to different sensitivities to metabolic inhibition triggered by hypoxia/ischemia. Regions of interest (CA1 or CA3) were selected from brightfield images prior to toxin exposure and propidium iodide treatment. Position registration marks were used so that each culture could be returned to the same position day-to-day for sequential measurements of fluorescence in each region of interest. On day 4, slices were exposed to 100 μ M NMDA that has been shown previously to kill 100 % of the neurons in these slices. Fluorescence intensity in each region of interest was expressed as a % of the final NMDA exposure.

Figure 6 shows examples of propidium iodide fluorescence images following exposure of organotypic slice cultures to 10 μ M, 100 μ M, or 1 mM MPP⁺. Within 1 day of exposure, there was a dose-dependent increase in propidium iodide fluorescence in the slice cultures. Little damage was observed following exposure to 10 μ M MPP⁺, whereas intense damage in CA1 and CA3 were observed within 2 days after exposure to 1 mM MPP⁺.

A remarkable finding was that there appeared to be selective vulnerability of CA1 vs CA3 to Complex I inhibition with MPP⁺ especially at the 1 mM dose. From day 1 to day 2, propidium iodide fluorescence increased from 51.5% to 91% in CA1 but only from 29.6% to

62% in CA3, with little further increase in either region after day 2. To our knowledge there have been no reports that complex I inhibition produces selective damage to hippocampal CA1 subfield similar to that commonly observed with hypoxia or ischemia.

Selective vulnerability of CA1 following Complex I inhibition was also observed following treatment with rotenone. The results are summarized in figures 7 and 8 that compare propidium iodide fluorescence in subfield CA1 and CA3 from organotypic slices exposed to different concentrations of rotenone. While cell death approached 100% in both CA1 and CA3 following exposure to 10 μ M rotenone, considerably less damage was seen in CA3 than in CA1 when the dose was reduced to 1.0 μ M. At a dose of 1.0 μ M, both the onset of damage and the degree of final damage were greater in CA1 and CA3. To date, we have not observed selective vulnerability of CA1 vs. CA3 following exposure to either 3-NP or NMDA. However, we have not yet run a sufficient number of doses for these agents to state conclusively whether they produce selective damage in cultured slices.

The topic of selective neuronal damage following exposure to mitochondrial toxins is an important one. If environmental agents (toxins) contribute to neuronal damage in neurodegenerative diseases, these agents must show selective toxicity to specific neuronal populations. It has always been difficult to understand how a general mitochondrial inhibitor, administered systemically, could selectively damage only a small population of neurons in the brain. Our data suggest that selective vulnerability to mitochondrial inhibition may be an intrinsic property of certain neurons. It would be interesting to compare sensitivity of other neuronal populations to mitochondrial inhibition *in vitro*. For example, are neurons in substantia nigra more sensitive to Complex I inhibition than neurons in hippocampus. If time permits in years 3 and 4 of this contract, we will attempt to examine this possibility.

4) Effect of toxins on mitochondrial membrane potential in brain slices

Mitochondrial depolarization has been linked to neuronal cell death both through loss of ATP production and necrosis, and through release of factors such as cytochrome c that may trigger apoptosis cascades. In these experiments we investigated mitochondrial depolarization in hippocampal slices following exposure to MPP⁺, 3-NP, NMDA, and rotenone. Changes in mitochondrial membrane potential were monitored with the fluorescent indicator JC-1 (5,5', 6,6'-tetrachloro-1,1',3,3'-tetraethylbenzimidazolecarbocyanide iodide). This dye partitions across membranes according to membrane potential. At high concentrations (large negative transmembrane potential) the dye forms aggregates which fluoresce at 590 nm, while at low concentrations (low transmembrane potential) the dye forms monomers which fluoresce at 535 nm. The ratio of 590/535 nm fluorescence can be used to indicate changes in mitochondrial membrane potential.

Hippocampal slices were loaded with JC-1 and fluorescence emission was detected from the CA1 subregion by microspectrofluorometry. Examples of emission spectra acquired after toxin treatment are shown in Figure 9. Each panel shows emission spectra acquired prior to toxin exposure, 30 min after exposure, and 60 min after exposure. A decrease in the ratio of 590 nm to 535 nm fluorescence indicates mitochondrial depolarization. The data are summarized in Figure 10 which shows the timecourse of changes in fluorescence emission ratios after toxin exposure. Control slices (ACSF) showed little change in mitochondrial membrane potential for more than 1 hr of measurement (Figs. 9A and 10). In contrast, 2 μ M CCCP (carbonyl cyanide m-chlorophenyl hydrazone), an uncoupler of mitochondrial respiration, caused rapid collapse of the mitochondrial membrane potential (Figs. 9B and 10).

MPP⁺ (1 mM), rotenone (10 μ M), 3-NP (1 mM) and NMDA (100 μ M) all caused some mitochondrial depolarization compared to control slices but none were as effective as CCCP. Of the four toxins tested, MPP⁺ produced the largest depolarization of mitochondrial membrane potential.

It is important to point out that these large doses of toxins all produced rapid inhibition of synaptic transmission and DC potential shifts signaling large changes in ion homeostasis. These data suggest that although the toxins inhibit ATP production, mitochondrial membrane potential (with the possible exception of MPP⁺) remains relatively intact. This may be explained by the fact that mitochondria will actually consume ATP to maintain the mitochondrial membrane potential under conditions when electron transport is compromised.

5) Effects of toxins on cytochrome c and Caspase 3 immunohistochemistry

An important question to be addressed by work funded as part of this contract is whether mitochondrial toxins trigger release of pro-apoptotic agents such as cytochrome c, and whether these agents activate apoptotic pathways involving Caspase-3. We proposed to use cell fractionation techniques and absorption spectrophotometry to monitor changes in cytochrome c. We have added western blot analysis and confocal immunocytochemistry of cytochrome c and active Caspase-3 to complement this method. Presented below (Figure 11) are preliminary data showing the effects of toxin exposure on the distribution of cytochrome c and Caspase-3 in sub-regions of hippocampal slices. Slices were exposed to either MPP⁺ (1 mM), rotenone (10 μ M), or NMDA (100 μ M) for 1 hr. Synaptic transmission was monitored to confirm a toxin effect. The slices were then fixed in paraformaldehyde and processed for confocal immunocytochemistry of cytochrome c (green fluorescence) and activated Caspase 3 (red fluorescence). Control slices showed a typical pattern of cytochrome c with punctate staining around the nucleus and in the neuropil indicating a mitochondrial distribution. This pattern was seen in CA1, CA3, and dentate gyrus (DG). No Caspase-positive cells were seen in any regions of control slices. MPP⁺ caused a decrease in cytochrome c immunofluorescence in CA1 with little change in CA3. In DG, cytochrome c appeared to be more uniformly distributed within the cytoplasm and many dentate granule cells were Caspase-3 positive. Rotenone produced large reductions in cytochrome c immunofluorescence both in CA1 and DG, but had little effect in CA3. Again, Caspase-positive cells were observed in DG after rotenone treatment, but not in CA1 or CA3. NMDA had little effect on either cytochrome c distribution or on activation of Caspase-3.

These data suggest that there may be toxin-induced changes in cytochrome c and Caspase-3 in hippocampus. However, it was surprising that no activation of Caspase-3 was observed in CA1, which by our other measurements appears to be selectively vulnerable to some of these mitochondrial inhibitors. It is important to point out, however, that the immunocytochemistry method only provides a snapshot in time of the changes occurring after toxin exposure. Moreover, the method is qualitative, showing changes in distribution but not in overall content. Future experiments will examine more time points and will be combined with cell fractionation and western blot analysis for quantitative comparisons. We will also employ these techniques using the organotypic slice cultures to examine more chronic time-points and for estimation of toxin-induced cell death.

Key Accomplishments

- Completed dose-response analysis of the effects of NMDA on synaptic transmission and mitochondrial NADH/NAD⁺ redox activity in hippocampal slices.
- Examined the effect of rotenone, a mitochondrial Complex I inhibitor and potential Parkinson's Disease toxin, on synaptic transmission and mitochondrial NADH redox activity.
- Compared the effects of MPP⁺, rotenone, 3-NP, and NMDA on cell viability in organotypic slice cultures of hippocampus.
- Discovered selective vulnerability of hippocampal CA1 neurons to mitochondrial Complex I inhibition with MPP⁺ and rotenone.
- Examined changes in mitochondrial membrane potential following exposure of hippocampal slices to MPP⁺, rotenone, 3-NP, and NMDA.
- Examined changes in cytochrome c and activated Caspase-3 distribution in hippocampal slices following exposure to mitochondrial toxins using confocal immunocytochemistry.

Reportable Outcomes

None completed to date.

Conclusions

The data acquired to date clearly show early changes in mitochondrial and electrophysiological function associated with exposure of hippocampal slices to inhibitors of respiratory chain Complex I (MPP⁺ and rotenone), Complex II (3-NP), and the excitotoxin NMDA. Moreover, exposure of organotypic slice cultures to these same agents resulted in hippocampal cell death with 1-2 days. A remarkable and novel finding was that Complex I inhibitors appeared to selectively damage cells in hippocampal subfield CA3. These cells are known to be selectively vulnerable to hypoxia/ischemia, but are thought not to be damaged in other neurodegenerative diseases such as Parkinson's disease. If environmental toxins play a significant role in neurodegenerative diseases, there must be specific mechanisms whereby some cells are vulnerable while others remain resistant. It will be important in future studies to determine the mechanisms of selective neuronal vulnerability to mitochondrial toxins. A first step might be to compare vulnerability of different cell types known to be involved in specific neurodegenerative diseases. For example, it would be valuable to compare sensitivity of nigral-striatal and hippocampal slices to Complex I inhibition with rotenone.

Our data suggest that changes in cytochrome c distribution may play a role in the neurodegeneration associated with inhibition of Complex I. However, we found no evidence that activation of Caspase-3 was involved in this toxicity. This data suggests that: 1) Caspase-3 induced apoptosis is not the mechanism by which CA1 pyramidal cells die after Complex I inhibition. 2) changes in cytochrome c distribution contribute to

cell death by another mechanism, perhaps necrosis. It remains possible that other apoptotic pathways are involved in the cell death associated with Complex I inhibition. To test this possibility we propose to repeat these experiments and examine activation of other factors including Caspase-8 and Caspase-9. Future studies will also focus on other pathways contributing to cell death following toxin exposure as outlined in our original Statement of Work. These include intracellular calcium ion homeostasis and formation of reactive oxygen species.

Appendices (11 Figures)

Figure Legends

Figure 1. Effect of N-methyl-d-aspartate (NMDA) on evoked potential amplitude recorded in hippocampal subfield CA1 following electrical stimulation of the Schaffer collaterals. N_2 represents evoked potential amplitude after anoxia. ANOVA indicated a highly significant dose effect of NMDA on evoked potential activity ($F = 14.7$, $p < .001$, $n = 5$). Post hoc Dunnett's analysis showed significant changes from ACSF treated controls 10-60 min after exposure to 50 or 100 μM NMDA (+ $p < .05$, * $p < .01$, ** $p < .001$).

Figure 2. Effect of N-methyl-d-aspartate (NMDA) on mitochondrial nicotinamide adenine dinucleotide (NADH) fluorescence in hippocampal slices. Fluorescence levels are expressed as % of the control level prior to drug administration. N_2 represents the NADH fluorescence level during anoxia. ANOVA indicated a significant dose effect of NMDA on NADH fluorescence ($F = 7.09$, $p < .01$, $n = 5$). Significant differences from control were observed for 50 and 100 μM NMDA 20-60 min following exposure (+ $p < .05$, * $p < .01$, ** $p < .001$).

Figure 3. Effect of rotenone on evoked potential amplitude recorded in hippocampal subfield CA1 following electrical stimulation of the Schaffer collaterals. N_2 represents evoked potential amplitude after anoxia. ANOVA indicated a significant dose effect of rotenone on evoked potential activity ($F = 7.7$, $p < .01$, $n = 5$). Dunnett's post-hoc analysis indicated a significant difference between ACSF-treated control slices and slices treated with 5 μM or 10 μM rotenone (+ $p < .05$, * $p < .01$, ** $p < .001$).

Figure 4. Effect of rotenone on mitochondrial nicotinamide adenine dinucleotide (NADH) fluorescence in hippocampal slices. Fluorescence levels are expressed as % of the control level prior to drug administration. N_2 represents the NADH fluorescence level during anoxia. ANOVA did not reveal any significant effect of rotenone on NADH fluorescence ($F = 0.06$, $p > .05$, $n = 5$). However, it appeared that rotenone inhibited the increase in fluorescence normally observed following nitrogen exposure. This latter effect, however did not reach statistical significance ($F = 2.7$, $p = .08$).

Figure 5. Effect of 1-methyl-4-phenylpyridium (MPP⁺) on mitochondrial nicotinamide adenine dinucleotide (NADH) fluorescence in hippocampal slices. Fluorescence levels are expressed as % of the control level prior to drug administration. N₂ represents the NADH fluorescence level during anoxia. MPP⁺ treatment resulted in a significant increase in NADH fluorescence ($F = 11.7$, $p < .01$, $n = 5$) compared to ACSF-treated control slices ($+ p < .05$, $* p < .01$, compared to ACSF, Dunnett's post-hoc analysis).

Figure 6. Examples of propidium iodide fluorescence in organotypic slice cultures of hippocampus after exposure to 1-methyl-4-phenylpyridium (MPP⁺). Slices were exposed to the indicated concentration of MPP⁺ on Day 0 after acquisition of the baseline image.

Figure 7. Quantitative analysis of propidium iodide fluorescence in hippocampal subfield CA1 after exposure to the indicated concentrations of rotenone. ANOVA indicated a significant main effect of drug dose ($F = 30.0$, $p < .001$, $n = 4$) and time following exposure ($F = 42.1$, $p < .001$, $n = 4$). Comparisons of drug-treated groups with vehicle-treated controls indicated significant increases in propidium iodide fluorescence (increased cell death) following treatment with 1.0 or 10 μ M rotenone, 1, 2, and 3 days following exposure ($+ p < .05$, $* p < .01$, $** p < .001$, Dunnett's post-hoc analysis).

Figure 8. Quantitative analysis of propidium iodide fluorescence in hippocampal subfield CA3 after exposure to the indicated concentrations of rotenone. ANOVA indicated a significant main effect of drug dose ($F = 48.6$, $p < .001$, $n = 4$) and time following exposure ($F = 10.9$, $p < .01$, $n = 4$). In contrast to effects observed in CA1, comparisons of drug-treated groups with vehicle-treated controls indicated no significant increases in propidium iodide fluorescence (increased cell death) following treatment with 1.0 μ M rotenone, 1 or 2 days following exposure. Significant increases in propidium iodide fluorescence were only observed 3 days following exposure to 1.0 μ M rotenone. Increased propidium iodide fluorescence was observed 1, 2, and 3 days following exposure to 10 μ M rotenone ($+ p < .05$, $* p < .01$, $** p < .001$, Dunnett's post-hoc analysis).

Figure 9. Fluorescence emission spectra of the mitochondrial membrane potential indicator JC-1. Spectra were acquired by rapid scanning microspectrofluorometry prior to, 30 min, and 60 min after toxin administration. A) Control, artificial cerebrospinal fluid, B) Uncoupling agent, carbonyl cyanide m-chlorophenyl hydrazone (CCCP), C) 1-methyl-4-phenylpyridium (MPP⁺), D) Rotenone (Rot), E) 3-nitropropionic acid (3-NP), F) N-methyl-d-aspartate (NMDA).

Figure 10. Timecourse of changes in JC-1 fluorescence ratio (590/535 nm) after toxin exposure ($n = 2$, insufficient for statistical analysis).

Figure 11. Confocal immunocytochemistry images of cytochrome c (green fluorescence) and activated Caspase-3 (red fluorescence) taken 1 hr after exposure to artificial cerebrospinal fluid (ACSF), 1 mM 1-methyl-4-phenylpyridium (MPP⁺), 10 μ M rotenone, or 100 μ M N-methyl-d-aspartate (NMDA). Images were acquired from hippocampal subfields CA1, CA3, and dentate gyrus (DG). Arrows indicate the presence of Caspase-3 positive neurons.

NMDA

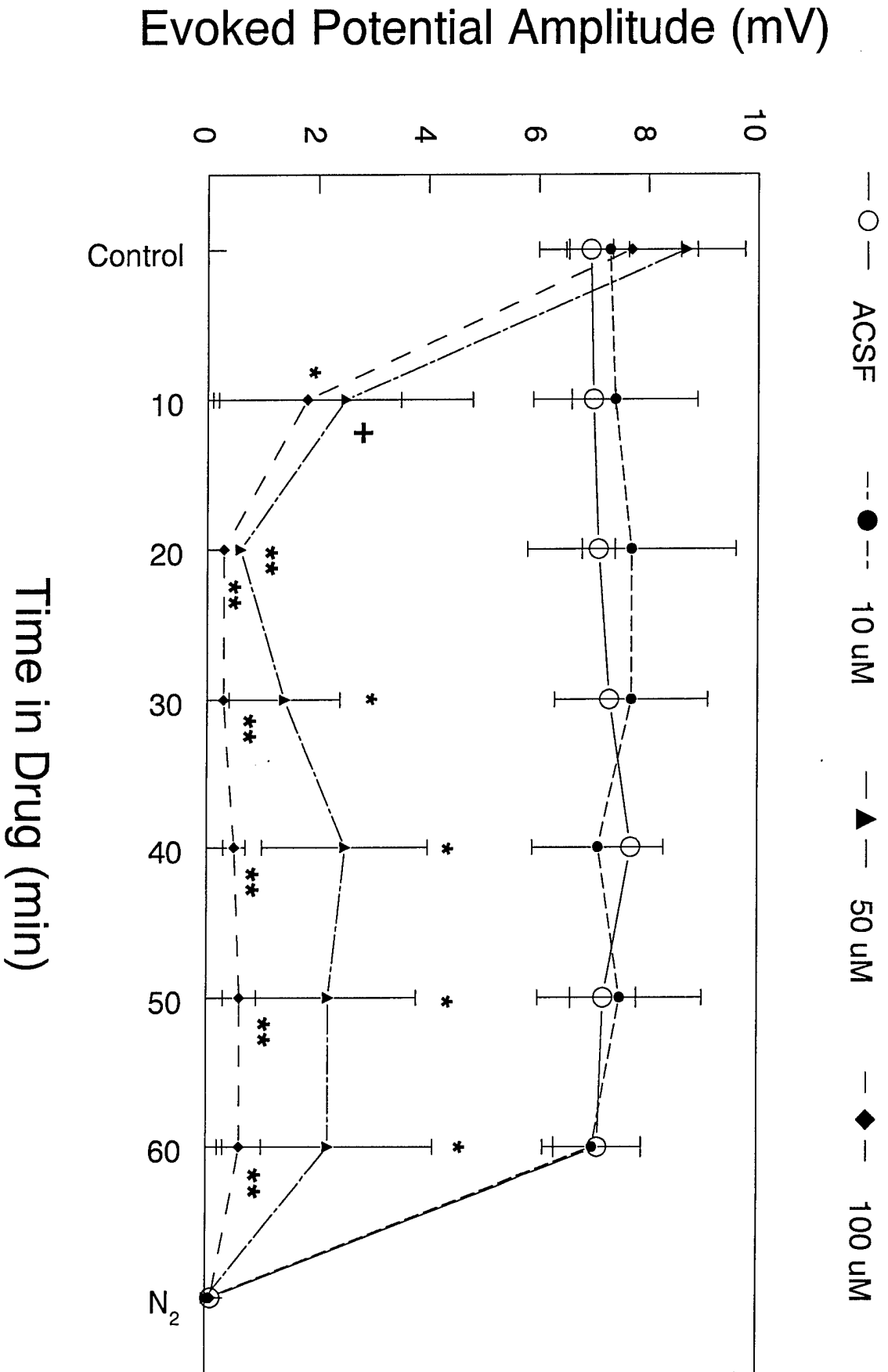


Figure 1

NMDA

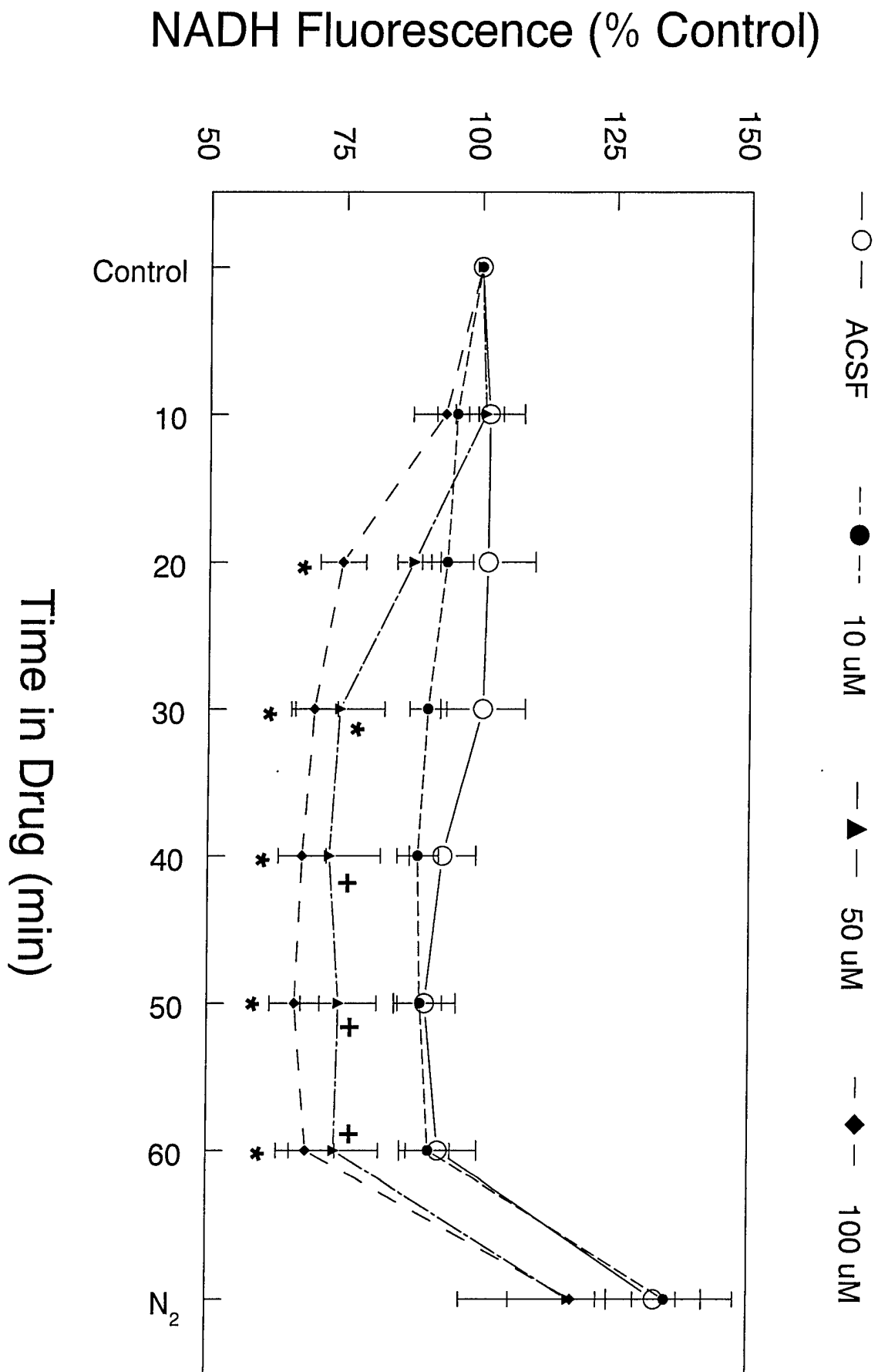


Figure 2

Rotenone

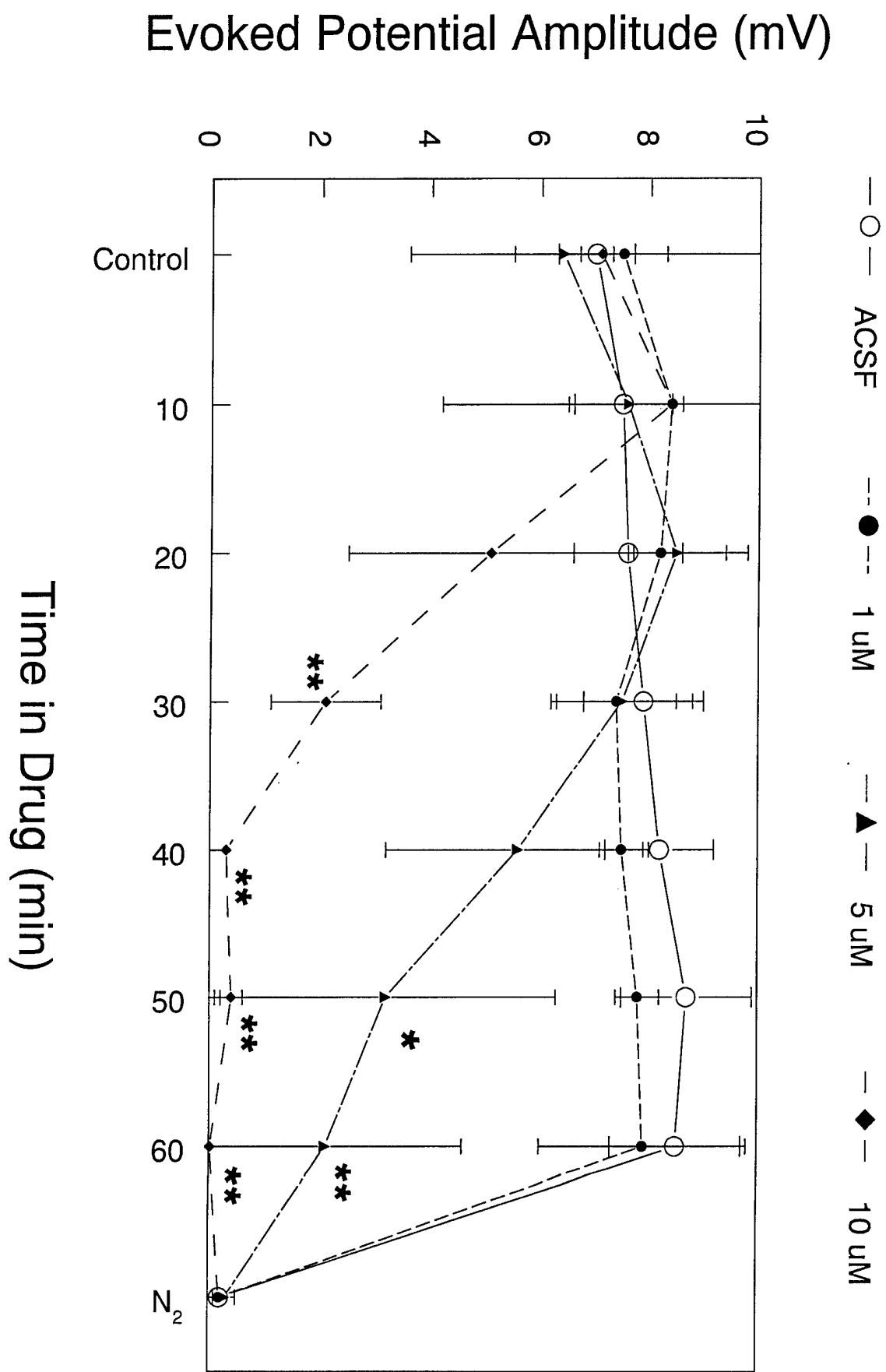


Figure 3

Rotenone

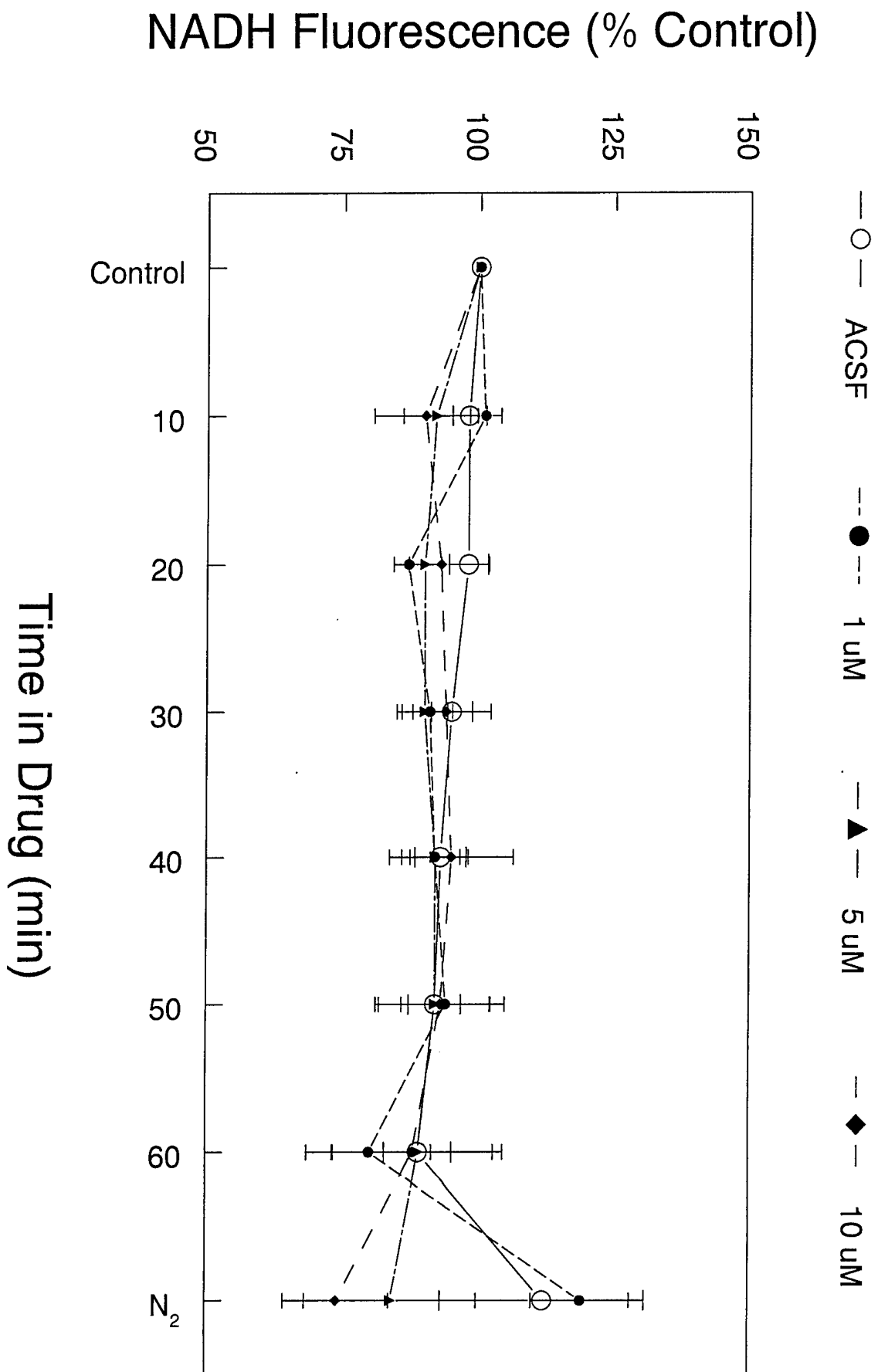


Figure 4

MPP⁺

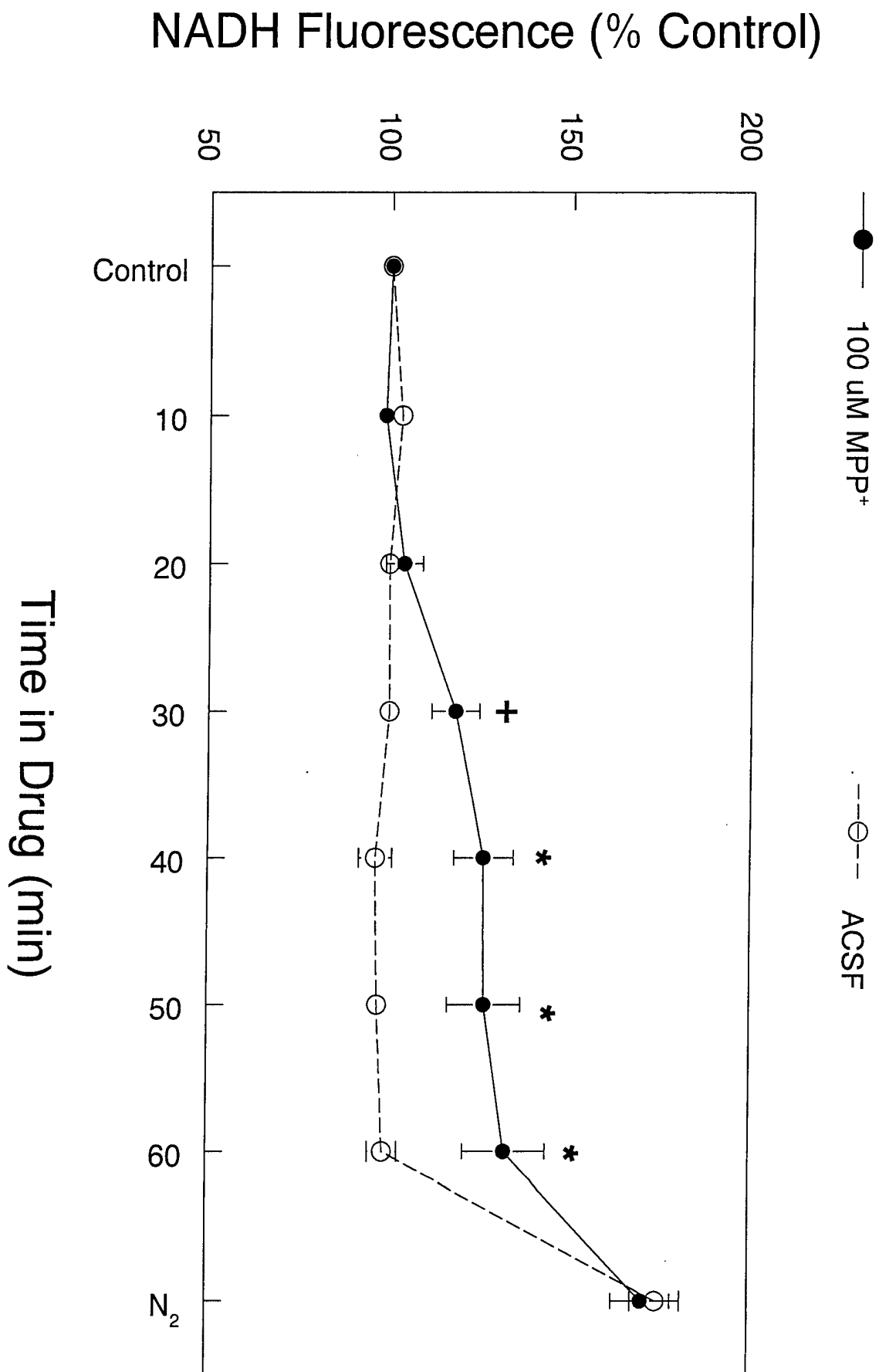


Figure 5

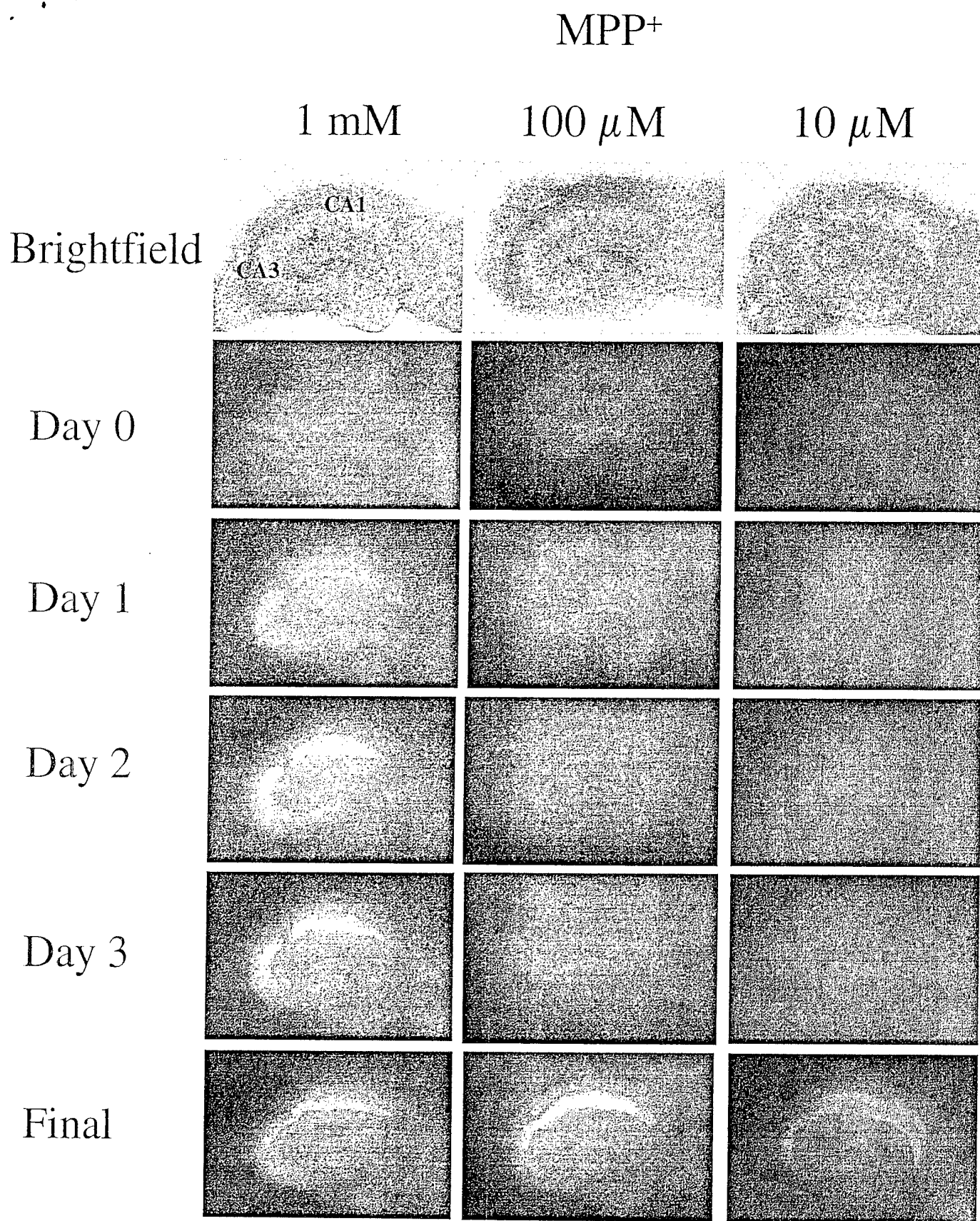
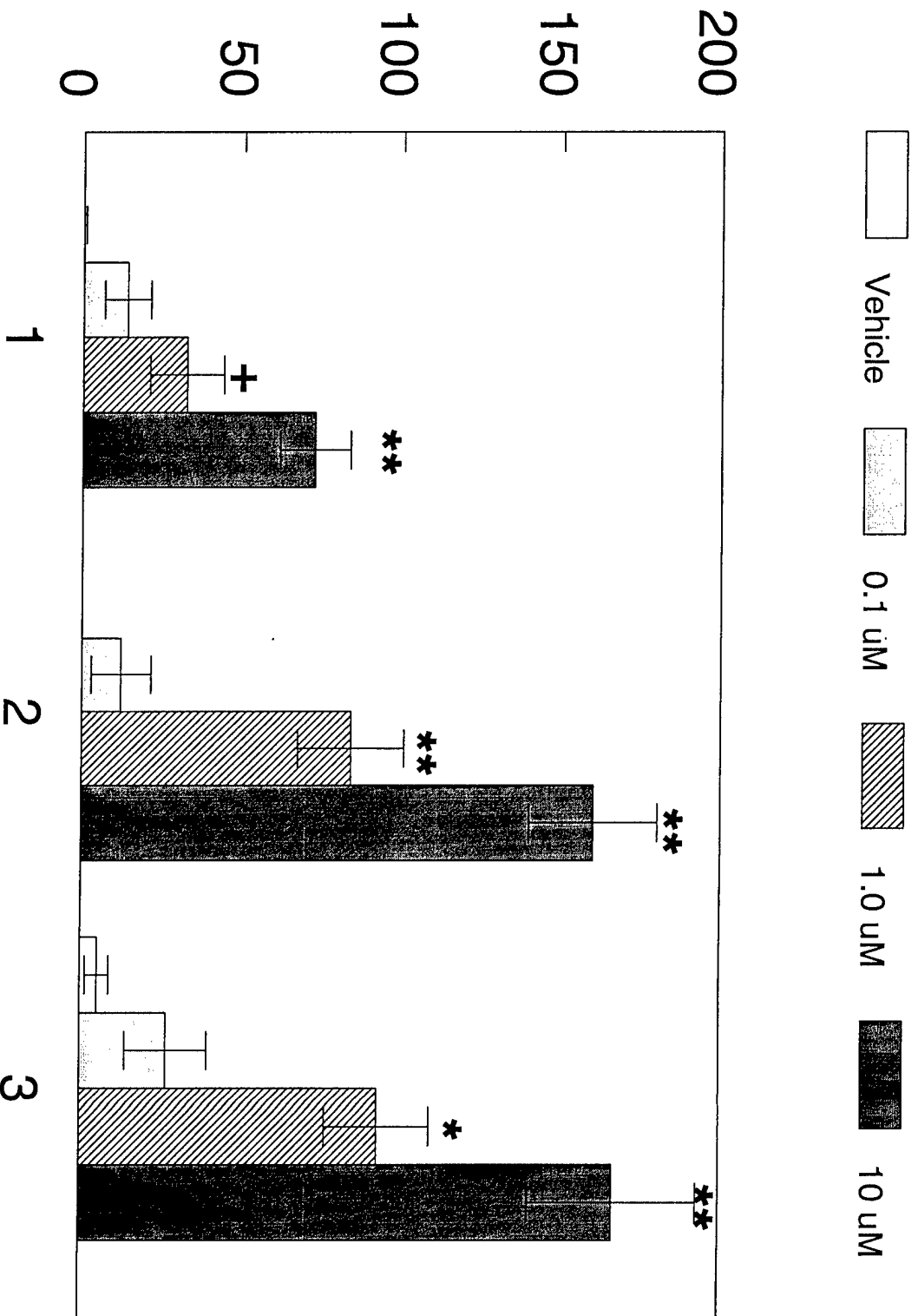


Figure 6

CA1

Propidium Iodide Fluorescence (% NMDA)

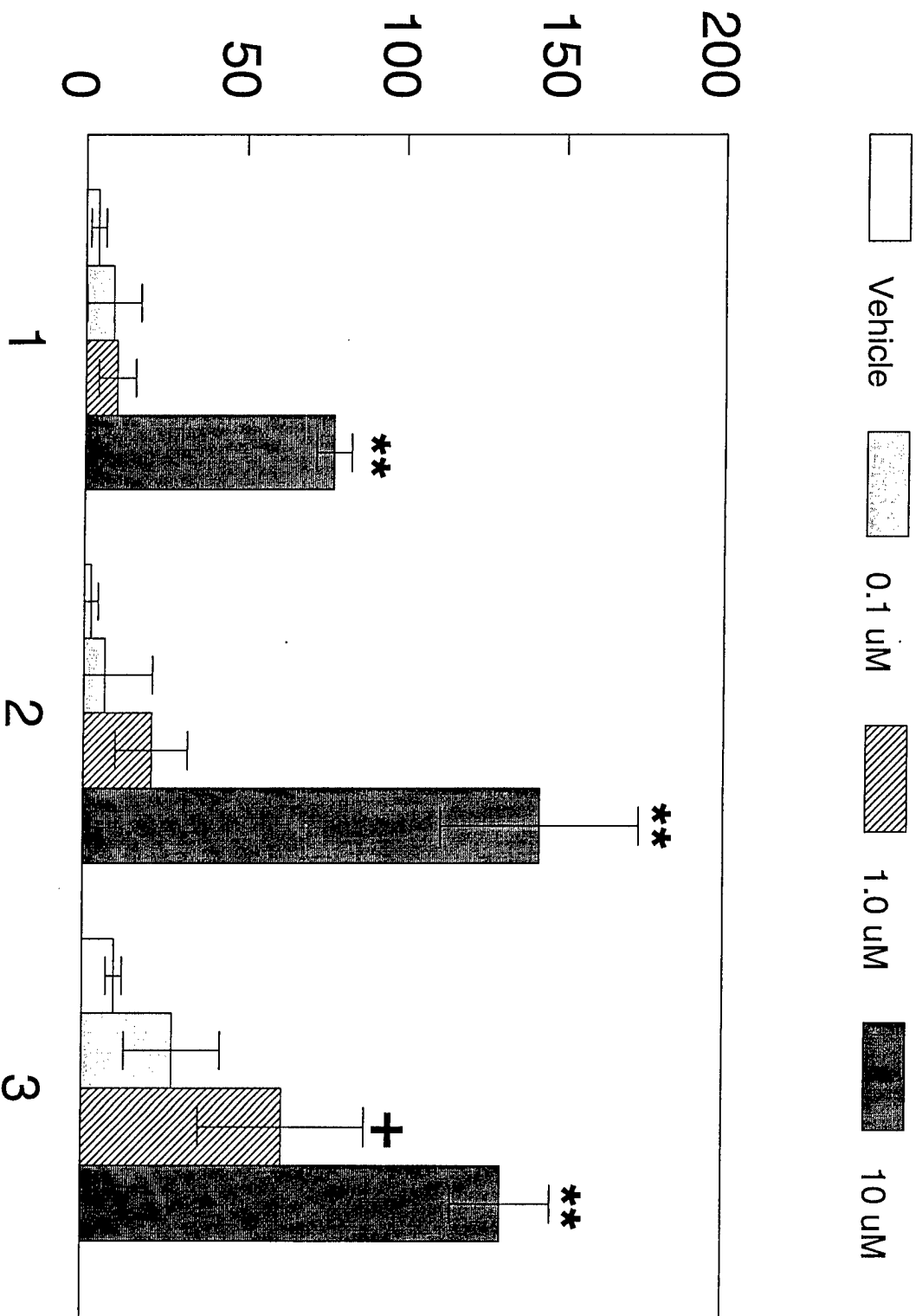


Days After Exposure

Figure 7

CA3

Propidium Iodide Fluorescence (% NMDA)



Days After Exposure

Figure 8

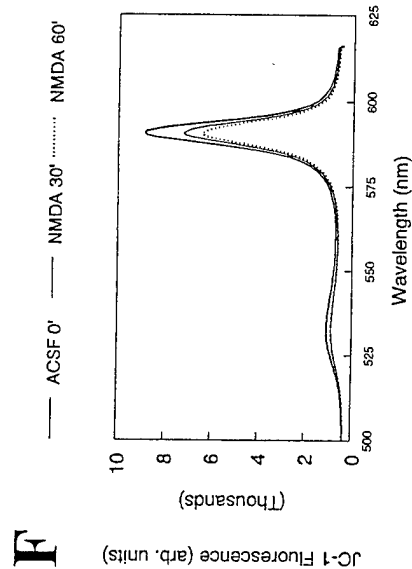
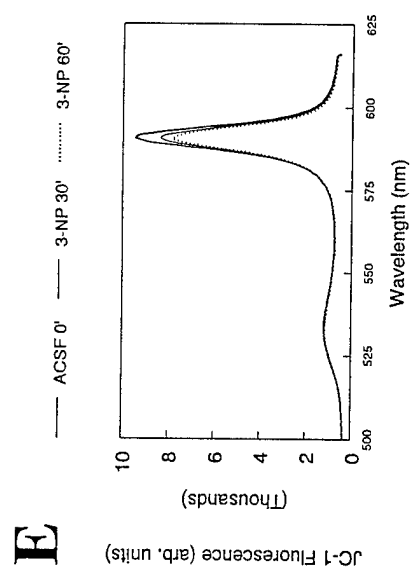
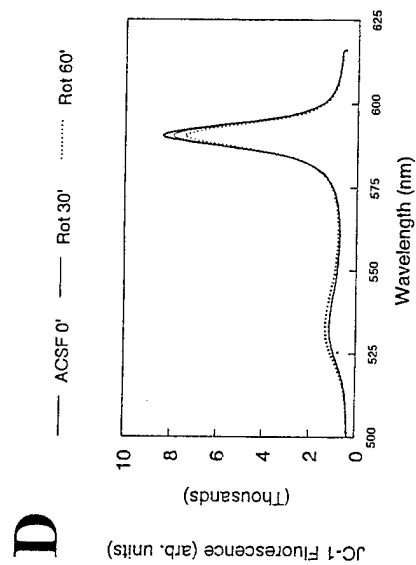
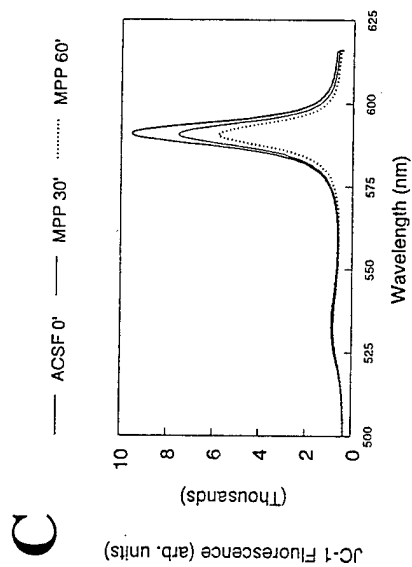
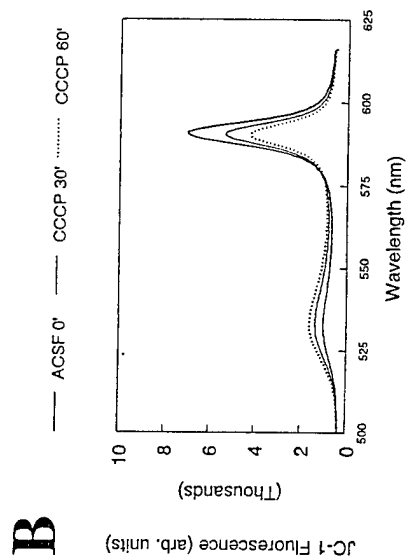
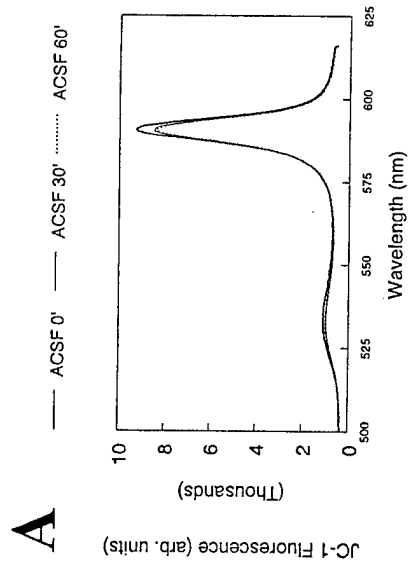
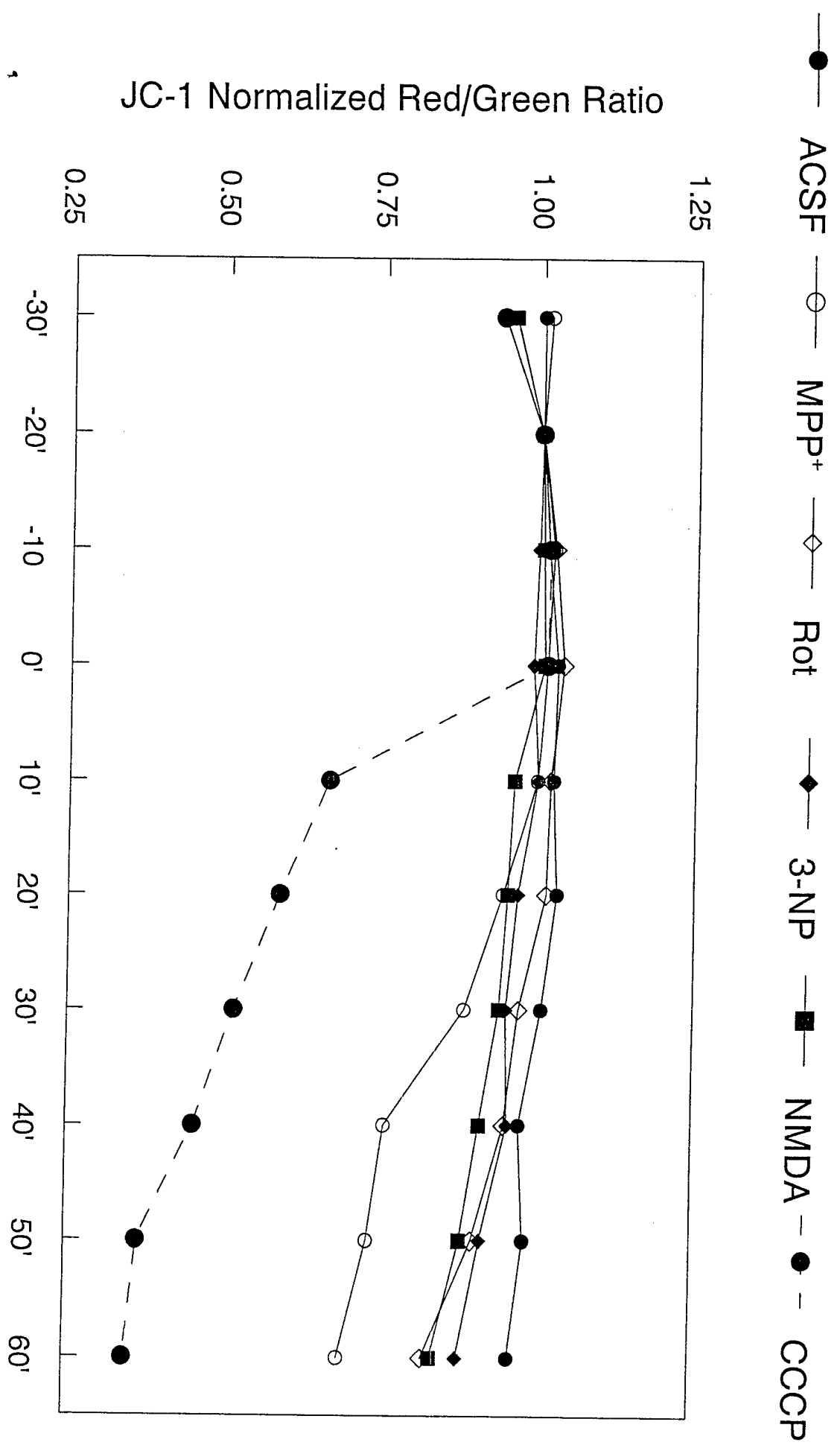


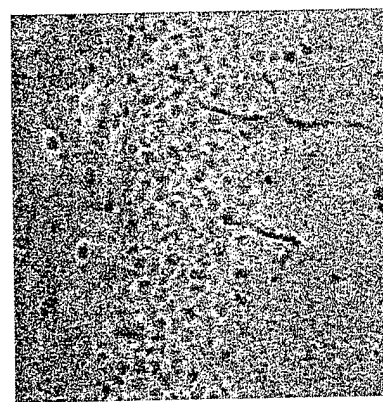
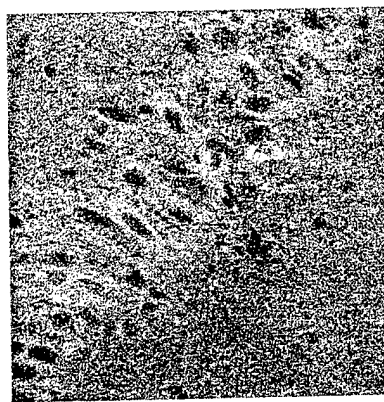
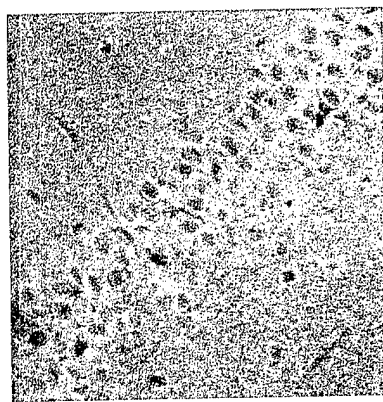
Figure 9



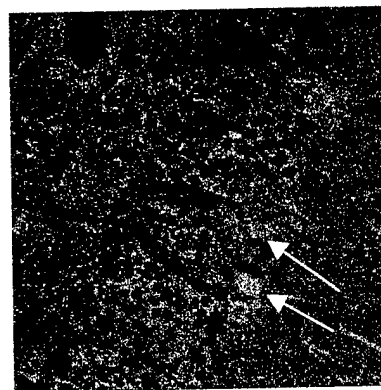
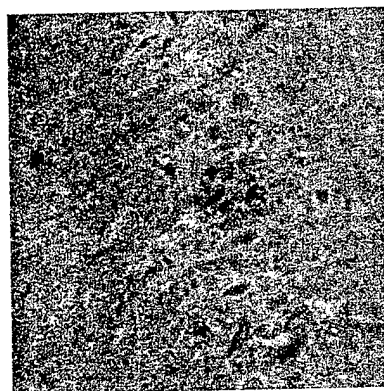
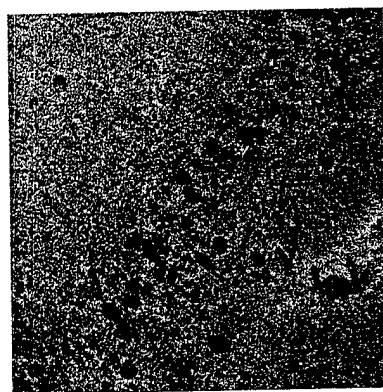
Time (min)

Figure 10

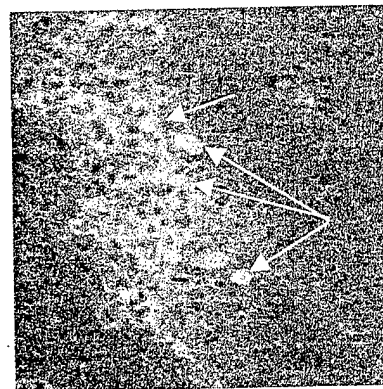
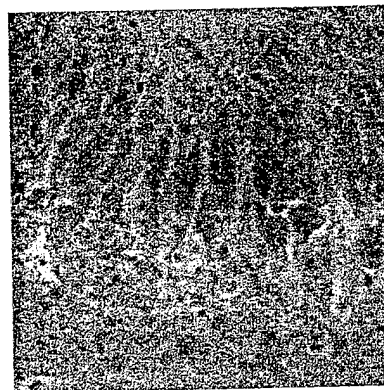
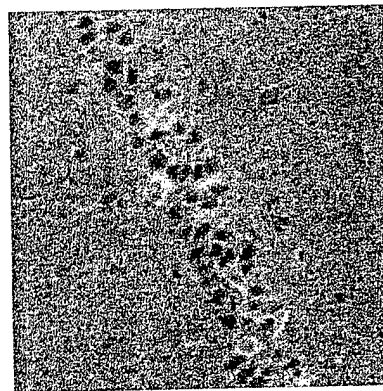
NMDA



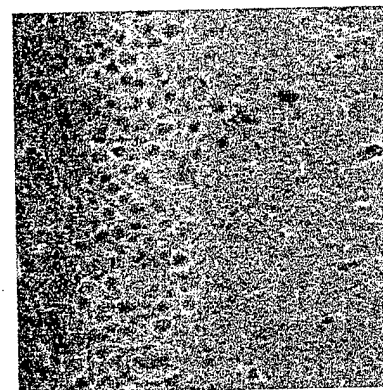
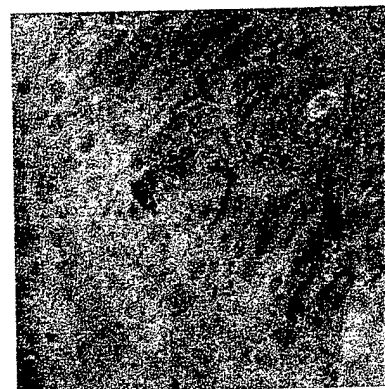
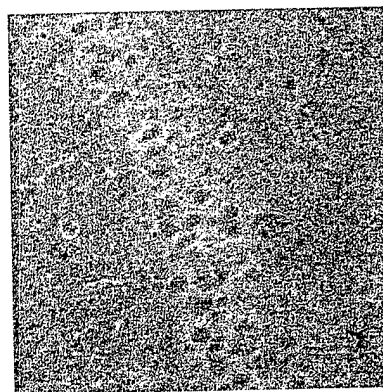
Rotenone



MPP+



ACSF



CA1

CA3

DG

Figure 11